J|A|C|S
ARTICLES
Published on Web 03/14/2003

^{1}H Fast MAS NMR Studies of Hydrogen-Bonding Interactions in Self-Assembled Monolayers

Shane Pawsey,[†] Mark McCormick,[‡] Susan De Paul,[‡] Robert Graf,[‡] Y. S. Lee,[†] Linda Reven,*[,†] and Hans W. Spiess*[,‡]

Contribution from the Department of Chemistry, McGill University, 801 Sherbrooke Street West, Montreal, Quebec, Canada H3A 2K6, and Max-Planck-Institut für Polymerforschung, Postfach 3148, D-55021 Mainz, Germany

Received October 18, 2002; E-mail: linda.reven@mcgill.ca

Abstract: The structures formed by the adsorption of carboxyalkylphosphonic acids on metal oxides were investigated by ^{1}H fast magic angle spinning (MAS), heteronuclear correlation (HETCOR), and ^{1}H double-quantum (DQ) MAS solid-state NMR experiments. The diacids $HO_2C(CH_2)_nPO_3H_2$ ($n = 2$, 3, 11, and 15) were adsorbed on TiO_2 and two types of ZrO_2 powders having average particle sizes of 20, 30, and 5 nm, respectively. Carboxyalkylphosphonic acids bind selectively via the phosphonate group, forming monolayers with pendant carboxylic acid groups. Whereas dipolar coupled P−OH protons are detected on TiO_2, there are only isolated residual P−OH groups on ZrO_2, reflecting the relative binding strengths of phosphonic acids on these two substrates. From a comparative ^{1}H MAS NMR study with an analogous monolayer system, $HO_2C(CH_2)_7SH$ coated gold nanoparticles, the hydrogen-bonding network at the monolayer/air interface is found to be quite disordered, at least for SAMs deposited on nonplanar substrates. Whereas only hydrogen-bonded homodimers occur in the bulk diacids, hydrogen bonding between the carboxylic and phosphonic acid groups is present in multilayers of the diacids on the ZrO_2 nanopowder.

1. Introduction

Self-assembled monolayers (SAMs) are widely used to introduce different chemical functionalities on metal and metal oxide substrates. With the exception of silanes on silica, the modification of metal oxide surfaces with SAMs is poorly developed. For metal oxides other than silica, long chain carboxylic acids have been the surfactants of choice to form SAMs, but there are relatively few studies as compared to the thiol/gold or silane/silica systems.[1] Limitations of the fatty acid SAMs include the stability of the surface bond which is ionic rather than covalent and the possibility of forming undesirable looping structures for surfactants of the type $X(CH_2)_nCO_2H$, where X is some other polar functionality.[1,2] Alkyl phosphonates and phosphonic acids present an attractive alternative because they bind more strongly than carboxylic acids to a wide range of metal oxides.[3−14] Phosphonic acids are commonly employed as corrosion inhibitors, adhesion promoters, and flotation agents to treat industrial materials and minerals containing alumina, iron, and tin.[11] Titanium surfaces have been modified with phosphonic acids to improve the bone binding of medical implants[15] and for photoelectrochemical cells based on polycrystalline titanium dioxide films.[16,17] More exotic metal oxides, such as tantalum and niobium oxides, have been derivatized with self-assembled monolayers of alkyl phosphonates for sensor development.[3−5]

We have recently shown that phosphonic acid based SAMs can be used to introduce polar functional groups on metal oxides.[14] ^{31}P and ^{13}C solid-state NMR and vibrational spectroscopic studies of carboxyalkylphosphonic acids, $HO_2C(CH_2)_nPO_3H_2$, deposited on TiO_2 and ZrO_2 powders demonstrate that the PO_3H_2 group binds preferentially, creating pendant carboxylic acid groups. This particular surfactant is an important test case as elemental analysis indicates a high degree of surface coverage, and spectroscopic data (^{13}C NMR and FT-IR) show that long chain carboxylic and phosphonic acids both form

[†] McGill University.
[‡] Max-Planck-Institut für Polymerforschung.

(1) Ulman, A. *Chem. Rev.* **1996**, *96*, 1533−54.
(2) Pawsey, S.; Yach, K.; Halla, J.; Reven, L. *Langmuir* **2000**, *16*, 3294−303.
(3) Brovelli, D.; Haehner, G.; Ruiz, L.; Hofer, R.; Kraus, G.; Waldner, A.; Schloesser, J.; Oroszlan, P.; Ehrat, M.; Spencer, N. D. *Langmuir* **1999**, *15*, 4324−7.
(4) Textor, M.; Ruiz, L.; Hofer, R.; Rossi, A.; Feldman, K.; Haehner, G.; Spencer, N. D. *Langmuir* **2000**, *16*, 3257−71.
(5) Hofer, R.; Textor, M.; Spencer, N. D. *Langmuir* **2001**, *17*, 4014−20.
(6) Woodward, J. T.; Ulman, A.; Schwartz, D. K. *Langmuir* **1996**, *12*, 3626−9.
(7) Woodward, J. T.; Schwartz, D. K. *J. Am. Chem. Soc.* **1996**, *118*, 7861−2.
(8) Woodward, J. T.; Doudevski, I.; Sikes, H. D.; Schwartz, D. K. *J. Phys. Chem. B* **1997**, *101*, 7535−41.
(9) Yee, C.; Kataby, G.; Ulman, A.; Prozorov, T.; White, H.; King, A.; Rafailovich, M.; Sokolov, J.; Gedanken, A. *Langmuir* **1999**, *15*, 7111−5.
(10) Shafi, K. V. P. M.; Ulman, A.; Yan, X.; Yang, N.-L.; Estournes, C.; White, H.; Rafailovich, M. *Langmuir* **2001**, *17*, 5093−7.
(11) Van Alsten, J. G. *Langmuir* **1999**, *15*, 7605−14.
(12) Gao, W.; Dickinson, L.; Grozinger, C.; Morin, F. G.; Reven, L. *Langmuir* **1997**, *13*, 115−8.
(13) Gao, W.; Dickinson, L.; Grozinger, C.; Morin, F. G.; Reven, L. *Langmuir* **1996**, *12*, 6429−35.
(14) Pawsey, S.; Yach, K.; Reven, L. *Langmuir* **2002**, *18*, 5205−12.
(15) Viornery, C.; Chevolot, Y.; Leonard, D.; Aronsson, B.-O.; Pechy, P.; Mathieu, H. J.; Descouts, P.; Graetzel, M. *Langmuir* **2002**, *18*, 2582−9.
(16) Zakeeruddin, S. M.; Nazeeruddin, M. K.; Pechy, P.; Rotzinger, F. P.; Humphry-Baker, R.; Kalyanasundaram, K.; Graetzel, M.; Shklover, V.; Haibach, T. *Inorg. Chem.* **1997**, *36*, 5937−46.
(17) Bonhote, P.; Moser, J.-E.; Humphry-Baker, R.; Vlachopoulos, N.; Zakeeruddin, S. M.; Walder, L.; Graetzel, M. *J. Am. Chem. Soc.* **1999**, *121*, 1324−36.

10.1021/ja029008u CCC: $25.00 **© 2003 American Chemical Society**

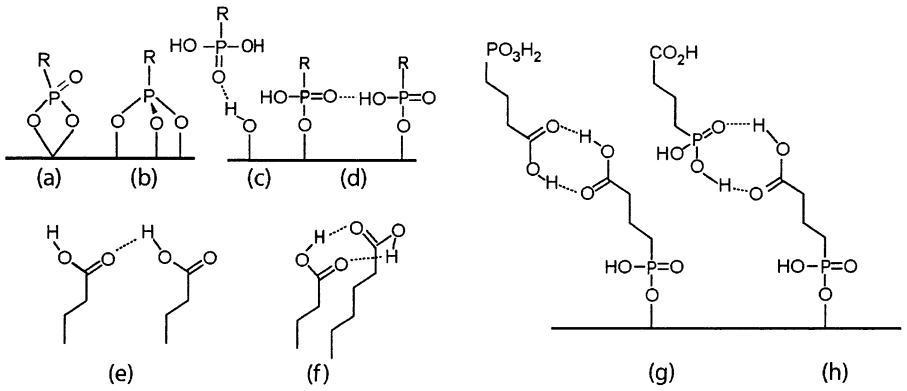

Figure 1. Schematic of some of the possible structures formed by the adsorption of $HO_2C(CH_2)_nPO_3H_2$. (a,b) The surface binding modes may be mono-, bi-, or tridentate in a bridging or chelating configuration. (c,d) Hydrogen-bonding interactions among the phosphate groups or with the surface hydroxyl groups are also possible. (e,f) Suggested hydrogen-bonding modes of the terminal CO_2H groups include acyclic linear hydrogen bonds[22] and distorted dimers.[23] (g,h) The hydrogen-bonding arrangement of the acid groups in multilayers may consist of homodimers and/or heterodimers.

densely packed monolayers with ordered alkane chains on ZrO_2.[2,12,13]

Carboxylic and phosphonic acids both form strong hydrogen bonds, and the nature of such phenomena at an interface is of interest in fields such as adhesion, chemical sensors, and bioseparations, among others. A great deal of effort has been expended to characterize hydrogen bonding at the monolayer/air interface of carboxylated organothiol SAMs on gold, which are extensively used for applications in electrochemistry, biology, and biomineralization. The measurements of true surface pK_a values[18] and the extent of hydrogen bonding at the air interface in these systems remain experimentally challenging.[19] Carboxyalkylphosphonate monolayers on a variety of metal oxide surfaces represent an analogous system to the carboxylated organothiol/Au SAMs, thereby providing another opportunity to study the hydrogen-bonding properties at the monolayer/air interface.

Vibrational spectroscopy has been the most useful method for detecting the presence or absence of hydrogen-bonding interactions in self-assembled monolayers. However, vibrational spectroscopy cannot directly give the structural details of the hydrogen-bonding network as provided by X-ray diffraction of bulk crystalline solids. With the development of techniques for detecting proton−proton proximities,[20,21] solid-state ^{1}H NMR spectroscopy presents an attractive alternative for characterizing hydrogen-bonding interactions in systems not amenable to X-ray diffraction and can provide more structural information than vibrational spectroscopy alone. ^{1}H detected NMR spectroscopy is also advantageous for surface studies. The high sensitivity and short relaxation times of protons as compared to nuclei with lower abundances and/or resonance frequencies enable longer experiments, such as relaxation measurements or two-dimensional NMR experiments, to be applied to surface-bound molecules.

In this paper, the structures formed by the adsorption of carboxyalkylphosphonic acids on metal oxide powders are characterized by ^{1}H fast magic-angle-spinning (MAS) NMR experiments. Some of the possible structures formed by the adsorption of $HO_2C(CH_2)_nPO_3H_2$ on TiO_2 and ZrO_2 are illustrated in Figure 1. The tridentate nature of the PO_3H_2 group gives rise to a large range of surface bonding possibilities such as mono-, bi-, or tridentate bonds in either a bridging or a chelating configuration (Figure 1a and b). In the event that P−OH groups are still present after adsorption, it would conceivably be possible for them to engage in hydrogen bonding with the metal oxide surface or among neighboring phosphate groups (Figure 1c and d). Additionally, it is also probable that remaining P−OH groups could engage in hydrogen bonding with μ-oxo oxygen atoms on the metal oxide surface (not shown).

For hydrogen-bonding interactions of the terminal acid groups of SAMs, linear hydrogen bonds[22] or distorted cyclic dimers[23] have both been proposed (Figure 1e and f). If more than a monolayer is adsorbed, the possible hydrogen-bonding arrangements of the excess diacid include head-to-head or head-to-tail configurations, as illustrated in Figure 1g and h. These possible structures were investigated using a combination of high-resolution ^{1}H solid-state NMR experiments. First, ^{1}H fast MAS NMR detects the presence of acid protons and allows an estimate of the hydrogen-bond strength based on the isotropic proton chemical shift. Second, 2D ^{1}H−X heteronuclear correlation (HETCOR) experiments (X = ^{31}P, ^{13}C) confirm the spectral assignments and identify heteronuclear through-space proximities. Finally, 2D ^{1}H double-quantum (DQ) MAS NMR gives more detailed spatial information by detecting dipolar connectivities and, by extension, the specific hydrogen-bonding interactions. These semiquantitative results, when added to the information from vibrational spectroscopy, provide a more complete picture of both the surface bonding and the hydrogen-bonding interactions in monolayers and multilayers on metal oxides. A quantitative determination of these structures, derived from density functional theory (DFT) calculations, will be presented in a later publication.[24]

2. Methods

2.1. Fast MAS ^{1}H NMR. Basic information about hydrogen bonding can be gained from the solid-state ^{1}H chemical shifts. The chemical shifts of acid protons have been empirically correlated to the hydrogen-

(18) Smalley, J. F.; Chalfant, K.; Feldberg, S. W.; Nahir, T. M.; Bowden, E. F. *J. Phys. Chem. B* **1999**, *103*, 1676−85.
(19) Arnold, R.; Azzam, W.; Terfort, A.; Woll, C. *Langmuir* **2002**, *18*, 3980−92.
(20) Schnell, I.; Spiess, H. W. *J. Magn. Reson.* **2001**, *151*, 153−227.
(21) Brown, S. P.; Spiess, H. W. *Chem. Rev.* **2001**, *101*, 4125−56.
(22) Leopold, M. C.; Black, J. A.; Bowden, E. F. *Langmuir* **2002**, *18*, 978−80.
(23) Smith, E. L.; Alves, C. A.; Anderegg, J. W.; Porter, M. D.; Siperko, L. M. *Langmuir* **1992**, *8*, 2707−14.
(24) McCormick, M.; Sebastiani, D.; Pawsey, S.; Reven, L.; Spiess, H. W. Unpublished results.

bond lengths in carboxylic and phosphonic acids.[25] Strong homonuclear dipolar couplings complicate the NMR spectroscopy of protons in rigid organic solids due to substantial broadening of the spectral lines, which typically obscures any chemical shift information. Previous studies of the proton chemical shifts in solid organic acids employed multipulse techniques that were complicated by a significant loss of signal, a disadvantage for surface studies. These experiments also require a tedious experimental setup to achieve maximum resolution and require corrections to the chemical shift scale due to partial averaging of the chemical shift interaction by the multipulse sequence.[25] These obstacles have been removed by the development of high-speed magic-angle-spinning (MAS) technology, and high-resolution solid-state NMR spectra of strongly dipolar-coupled spins are now routinely obtained using spinning frequencies of 25−30 kHz. In addition to information from the proton chemical shift, variable temperature ^{1}H MAS NMR allows the dynamics of hydrogen-bond breaking/formation to be followed in systems undergoing thermal transitions.

2.2. 2D ^{1}H−X Heteronuclear Correlation (HETCOR) NMR. The assignment of the acidic proton resonances is problematic for carboxyalkylphosphonic acids in both the bulk and the adsorbed states. The proton chemical shift ranges of hydrogen-bonded carboxylic and phosphonic acids in the solid-state overlap extensively, ranging between 12 and 20 ppm for carboxylic acids and 11−17 ppm for phosphonic acids.[25] Furthermore, assignment of the resonances of adsorbed organic acids cannot be based on the bulk state ^{1}H chemical shifts. Factors such as the amount of adsorbed water, the extent of hydrogen bonding between the surface-bound acid groups, and the possibility of the substrate acting as a hydrogen-bond acceptor all have an effect on the ^{1}H chemical shifts that will not be observed in the bulk acid. Fortunately, ^{31}P and ^{13}C NMR can be combined with fast MAS ^{1}H NMR for 2D ^{1}H−X HETCOR NMR experiments to assign the CO_2H and PO_3H_2 proton resonances. The 2D HETCOR experiments employed here use simple Hartmann−Hahn ^{1}H−X cross polarization which provided sufficient sensitivity for ^{31}P detection for all of the surface samples. Proton spin diffusion, which is present to some extent even under very fast MAS, leads to spatial equilibration of the proton magnetization and correlations between more distant spins in the HETCOR spectra. Therefore, short and long cross polarization contact times were used respectively to minimize and maximize proton spin diffusion for identifying shorter- and longer-range spatial correlations.

2.3. ^{1}H Double-Quantum (DQ) MAS NMR. In recent years, noncovalent interactions in macromolecular and supramolecular systems have been studied by a variety of high-resolution homonuclear and heteronuclear multiple quantum (MQ) solid-state NMR techniques based on through-space dipolar interactions between nuclei.[20,21] The largest MQ signals arise from strongly dipolar-coupled protons. Because the dipolar interaction is averaged by fast MAS, it must be reintroduced by a suitable pulse sequence to simultaneously detect strong ^{1}H−^{1}H dipolar couplings and enhance the ^{1}H chemical shift resolution. Robust recoupling pulse sequences for the efficient generation of multiple quantum coherences in the presence of fast MAS have been developed, allowing semiquantitative measurement of proton−proton proximities via 2D ^{1}H double-quantum (DQ) MAS solid-state NMR experiments.[20,21] The detection of a DQ signal indicates the presence of a dipole−dipole coupling between pairs of protons, and the absence of such a signal is due to either large ^{1}H−^{1}H distances or molecular motions on the time scale of the experiment (<100 μs). Short-range interactions, such as hydrogen-bonding or aromatic $\pi-\pi$ interactions, can be probed because this experiment is sensitive to ^{1}H−^{1}H distances of less than 0.35 nm. For example, the dimerization of carboxylic acid groups in liquid crystalline hexabenzocoronene carboxylic derivatives was followed by variable temperature ^{1}H DQ MAS NMR.[26] This experiment has proven to be particularly useful in cases where single crystals are not available and should likewise be effective for detecting hydrogen-bonding and other intermolecular interactions of surface-bound molecules.

3. Experimental Section

Materials. $HO_2C(CH_2)_2PO_3H_2$ and $HO_2C(CH_2)_3PO_3H_2$ were obtained from Lancaster Synthesis Inc. and were used without any further purification, while $HO_2C(CH_2)_{11}PO_3H_2$ and $HO_2C(CH_2)_{15}PO_3H_2$ were synthesized. All other reagents were obtained from Aldrich Chemical Co. unless noted otherwise. Starting with either 12-hydroxydodecanoic or 16-hydroxyhexadecanoic acid, we protected the carboxylic acid group through the formation of an ethyl ester by refluxing in absolute ethanol with 0.1 equiv of acetyl chloride. The resulting ester was brominated by refluxing in a methylene chloride solution with 1.05 equiv of *N*-bromosuccinimide and 1.1 equiv of triphenylphosphine. The resulting brominated ester was phosphonated with triethyl phosphite by the Michaelis−Arbazov reaction. The product $[(H_3CH_2CO)_2OP(CH_2)_xCO_2CH_2CH_3]$ was then hydrolyzed by refluxing in a concentrated HCl solution for a period of several days. The samples were purified by multiple recrystallizations.

Nonporous zirconia powder (VP zirconium dioxide, Degussa Corp.) was calcinated at 400 °C overnight before use to remove the residual organics that contaminated its ^{13}C NMR spectra. The reported average particle size is 30 nm with a BET surface area of 40 m^2/g. Titania powder (titanium dioxide P25, Degussa Corp.) with a reported average particle size of 21 nm and a specific surface area of 50 m^2/g was used without further modification. Nanocrystalline zirconia (ZrO_2) powder (separated equiaxial single crystals, cubic zirconium dioxide, Advanced Powder Technology Pty. Ltd.) had a reported particle size of 5 nm and a BET surface area of 140 m^2/g. The nanocrystalline zirconia powder was used without any further modification. The TiO_2 and nanocrystalline ZrO_2 showed no signs of organic contamination by ^{13}C NMR and as such were not calcinated. It is anticipated that the heating of the nonporous ZrO_2 will lower the concentration of hydroxyl groups on the surface of the metal oxide, but no controlled studies were performed to monitor its effect.

Sample Preparation. Adsorbed samples were prepared by dispersing 0.5 g of the metal oxide substrates in 150−200 mL of acetone with sonication. A solution of the carboxyalkylphosphonic acid containing 2.5 times excess what is necessary to form a monolayer was prepared in acetone with vigorous mixing. The well-dispersed substrate was mixed into the solution of carboxyalkylphosphonic acid and left to reflux with stirring for 2 days followed by an additional 2 days of annealing. The solids were separated from the solution by centrifugation and then filtering. The solid was thoroughly washed and filtered an additional five times in an attempt to remove any weakly bound surfactant and finally dried under vacuum. Because of the solubility of $HO_2C(CH_2)_{11}PO_3H_2$ as compared to the other carboxyalkylphosphonic acids, some samples underwent additional washing steps with hot methanol. The $HO_2C(CH_2)_7SH$/Au nanoparticles were prepared as described in an earlier study.[27]

Elemental Analysis. Elemental analysis and calculated coverages for the carboxyalkylphosphonic acid/metal oxide samples that were reported previously[14] are reproduced here in Table 1. The coverages were calculated by assuming that each molecule occupies 24 Å^2, based on the size of the PO_3H_2 group.

Solid-State NMR Spectroscopy. Single- and double-quantum ^{1}H MAS NMR spectra were acquired either on a Bruker ASX500 or on a DRX700 spectrometer equipped with a 2.5 mm fast MAS probe. The single-quantum ^{1}H MAS NMR spectra were acquired with a spinning frequency of 30 or 25 kHz using a Hahn echo sequence to suppress the broad proton background signal from the probe. The back-to-back

(25) Harris, R. K.; Jackson, P.; Merwin, L. H.; Say, B. J. *J. Chem. Soc., Faraday Trans. 1* **1988**, *84*, 3649−72.
(26) Brown, S. P.; Schnell, I.; Brand, J. D.; Müllen, K.; Spiess, H. W. *Phys. Chem. Chem. Phys.* **2000**, *2*, 1735−45.
(27) Schmitt, H.; Badia, A.; Dickinson, L.; Reven, L.; Lennox, R. B. *Adv. Mater.* **1998**, *10*, 475−80.

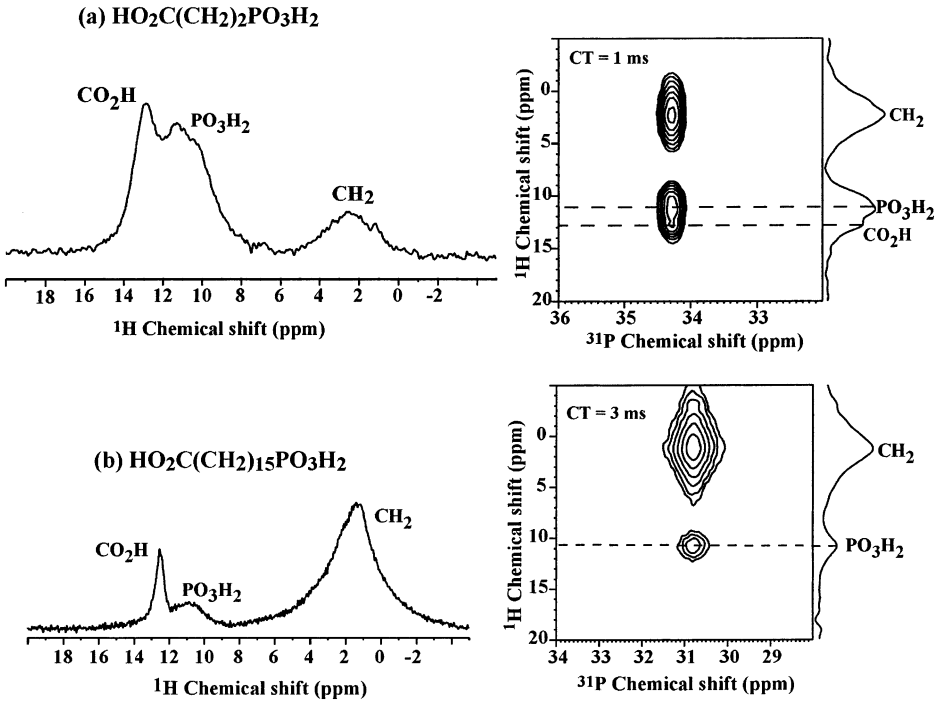

Figure 2. 1D ^{1}H DQ MAS and 2D ^{1}H−^{31}P HETCOR NMR spectra of (a) $HO_2C(CH_2)_2PO_3H_2$ and (b) $HO_2C(CH_2)_{15}PO_3H_2$ acquired with MAS spinning frequencies of 30 kHz. The DQ excitation time was 66 μs. Contact times of 1 and 3 ms are shown for the HETCOR spectra of $HO_2C(CH_2)_2PO_3H_2$ and $HO_2C(CH_2)_{15}PO_3H_2$, respectively.

Table 1. Samples and Estimated Coverage from Elemental Analysis

surfactant $HO_2C(CH_2)_nPO_3H_2$	substrate	coverage
$n = 2$	nanoZrO_2	248%
$n = 3$	nanoZrO_2	182%
$n = 11$	nanoZrO_2	104/80%[a]
$n = 15$	nanoZrO_2	103%
$n = 11$	ZrO_2	90%
$n = 15$	ZrO_2	94%
$n = 2$	TiO_2	82%
$n = 3$	TiO_2	73%
$n = 11$	TiO_2	90%
$n = 15$	TiO_2	94%

[a] Coverage after the $HO_2C(CH_2)_{11}PO_3H_2$ nanoZrO_2 sample was subjected to additional washings with hot methanol.

(BABA) recoupling pulse sequence,[28,29] which efficiently generates double-quantum coherences in the presence of very fast MAS, was used to acquire 1D and 2D DQ ^{1}H MAS NMR spectra with excitation times of one or two rotor periods. The 2D ^{1}H−^{31}P and ^{1}H−^{13}C heteronuclear correlation (HETCOR) NMR spectra were acquired at spinning frequencies of 25 or 30 kHz using ramped polarization transfer and contact times ranging from 100 μs to 5 ms.

4. Results

The characterization of the hydrogen-bonding interactions of bulk and adsorbed $HO_2C(CH_2)_nPO_3H_2$ as a function of chain length, substrate composition, and substrate particle size is presented in this section. The NMR methods described above were combined to assign chemical shifts, estimate the hydrogen-bond lengths, and detect dipolar connectivities. The bulk diacids are examined first as a function of chain length to determine the nature of the hydrogen bonds and to test the effectiveness of the HETCOR experiment for assignment of the acid proton chemical shifts. Next the results for the diacids adsorbed on two different lower surface area metal oxide powders, TiO_2 and ZrO_2, which should contain mainly *intramonolayer* rather than *intraparticle* hydrogen bonds, are described. These results are compared to an analogous system, $HO_2C(CH_2)_7SH$ monolayers on gold nanoparticles, which displays ^{1}H NMR spectra in appearance similar to that of the carboxyalkylphosphonate monolayers. This comparison was found to be useful for interpretation of the ^{1}H NMR results for the adsorbed diacids because the possibility of interactions of the terminal CO_2H groups with the gold substrate is excluded, and yet the small average gold particle size (∼2 nm diam) allows for *intraparticle* hydrogen bonds. Finally, the hydrogen bonding in multilayers formed by the adsorption of the diacids on a nanoparticle metal oxide substrate, ZrO_2 nanopowder (∼5 nm diam), is compared to that of the bulk diacids and the monolayers.

4.1. Bulk State Diacids: $HO_2C(CH_2)_nPO_3H_2$. The 1D double-quantum filter (DQF) ^{1}H MAS and 2D ^{1}H−^{31}P HETCOR NMR spectra of the longest and shortest chain diacids, $HO_2C(CH_2)_nPO_3H_2$, $n = 2$ and 15, are given in Figure 2. The double-quantum filter effectively suppresses the adsorbed water signals of the carboxyalkylphosphonic acids. The short chain diacids, $n = 2$ and 3, are especially hydroscopic and still showed a water signal even after drying overnight under vacuum. An excitation time of two rotor periods (66 μs) was used to enhance the DQ signals of the acid protons, which have much weaker dipolar couplings as compared to those of the methylene protons. In addition to the broad resonance at ∼1−2 ppm for the aliphatic protons, there are two resonances for the acidic protons. The positions and line widths of the two acidic proton peaks varied with the water content, approaching the shifts of 11 and 13.0 ppm after drying. Because the ^{1}H chemical shift ranges of

(28) Feike, M.; Demco, D. E.; Graf, R.; Gottwald, J.; Hafner, S.; Spiess, H. W. *J. Magn. Reson., Ser. A* **1996**, *122*, 214−21.
(29) Sommer, W.; Gottwald, J.; Demco, D. E.; Spiess, H. W. *J. Magn. Reson., Ser. A* **1995**, *113*, 131−4.

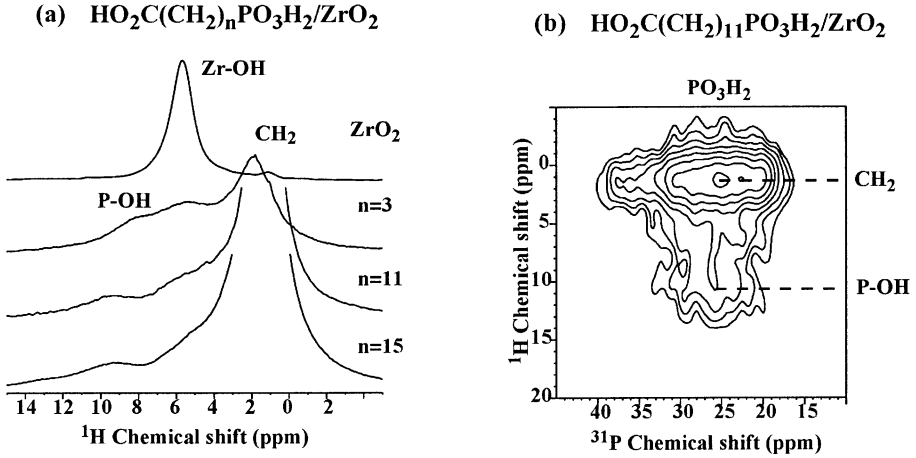

Figure 3. (a) 1D ^{1}H MAS NMR spectra of ZrO_2 powder and $HO_2C(CH_2)_nPO_3H_2$, $n = 3$, 11, 15, adsorbed on ZrO_2. (b) 2D ^{1}H$-^{31}$P HETCOR NMR spectrum of $HO_2C(CH_2)_{11}PO_3H_2$ adsorbed on ZrO_2. A contact time of 100 μs was used for the HETCOR spectrum.

carboxylic and phosphonic acid protons overlap,[16] ^{1}H$-^{31}$P HETCOR NMR spectra were acquired. Short contact times of 100 μs (not shown) were used to minimize proton spin diffusion. At the short contact time, there is only a correlation of the phosphate group to the peak at 11 ppm for both the short and the long chain diacids. The broad proton resonance at 11 ppm is thus assigned to the PO_3H_2 group, and the other acid proton resonance at ~13 ppm is assigned to the CO_2H proton. The isotropic proton chemical shifts can be empirically correlated with the hydrogen-bond length, r_{O-O}.[25] The shifts for the CO_2H and PO_3H_2 protons correspond to hydrogen-bond lengths of 2.66 and 2.63 Å, respectively.

Note that a shoulder at 13 ppm in the ^{1}H dimension of the HETCOR spectrum is present at longer contact times for the short chain diacid, $n = 2$, but not for the long chain, $n = 15$. Apparently the distance between the two acid groups in the long chain diacids is sufficient to prevent the development of a correlation between the phosphonate group and the carboxylic acid protons by spin diffusion, even for contact times as long as 5 ms. The resonances for the PO_3H_2 groups in the ^{1}H NMR spectra of the bulk diacids are notably broader than those of the CO_2H groups. The larger line width may reflect a more disordered or complex hydrogen-bonding network among the PO_3H_2 groups. The phosphonic acid group can act as both a hydrogen-bond donor through the two P$-$OH groups and an acceptor via the P═O oxygen. This tridentate character of the PO_3H_2 group can naturally lead to more complex hydrogen-bonded structures.

4.2. $HO_2C(CH_2)_nPO_3H_2$ on ZrO_2 and TiO_2 Powders. The ^{1}H fast MAS NMR spectra of the nonporous ZrO_2 powder (s.a. ≈ 40 m^2/g) and $HO_2C(CH_2)_nPO_3H_2$, $n = 3$, 11, and 15, adsorbed on the ZrO_2 powder are given in Figure 3a. The ZrO_2 powder consists of a broad resonance at ~6 ppm, assigned to the protons from the surface hydroxyl groups. The $HO_2C(CH_2)_nPO_3H_2/ZrO_2$ samples display the aliphatic resonance at ~1 ppm, a weak Zr$-$OH peak at 6 ppm, and a weak broad resonance centered at ~8$-$10 ppm. The weak peaks at ~8$-$10 ppm were not detected in the ^{1}H DQF MAS NMR spectra. A 2D ^{1}H$-^{13}$P HETCOR NMR spectrum, given in Figure 3b, shows that this peak is due to P$-$OH groups rather than the carboxylic acid protons. The signal sensitivity of this sample is insufficient for a ^{1}H$-^{13}$C HETCOR NMR experiment. However, any possibility that the weak 8$-$10 ppm ^{1}H peak is due to carboxylic acid protons can be ruled out from the ^{1}H$-^{31}$P HETCOR NMR experiments on the bulk long chain diacids, which showed that the phosphonic acid group and CO_2H protons are too far apart for a correlation to develop. Furthermore, the ^{1}H MAS NMR spectrum of octadecylphosphonic acid on ZrO_2 (not shown) also contains a very weak broad peak at ~8$-$10 ppm. The infrared spectra of the $HO_2C(CH_2)_nPO_3H_2/ZrO_2$ samples all have a strong band at ~1710 cm^{-1}, assigned to hydrogen-bonded carboxylic acid groups, and no bands attributable to the formation of surface zirconium carboxylate bonds.[14] However, the ^{1}H NMR signals of these pendant carboxylic acid groups appear to be broadened beyond detection.

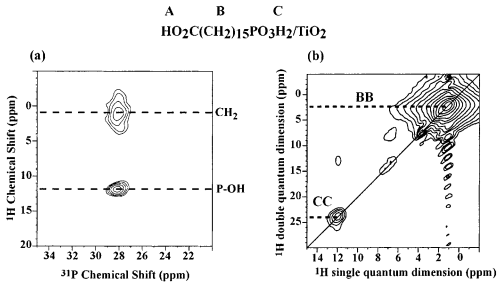

Figure 4. (a) 2D ^{1}H$-^{31}$P HETCOR NMR and (b) 2D ^{1}H DQ NMR spectra of $HO_2C(CH_2)_{15}PO_3H_2$ adsorbed on TiO_2 acquired at MAS spinning frequencies of 30 kHz. A contact time of 100 μs was used for the HETCOR spectrum, and the DQ excitation time was 66 μs.

The ^{1}H MAS NMR spectra of the $HO_2C(CH_2)_nPO_3H_2/TiO_2$ samples, not shown, contain a resonance at 12 ppm in addition to the aliphatic peak at 1 ppm. On the basis of the ^{1}H$-^{31}$P HETCOR NMR spectrum shown in Figure 4a, this peak is assigned to P$-$OH protons rather than to the pendant CO_2H groups. The ^{1}H MAS NMR spectrum of octadecylphosphonic acid on TiO_2 (not shown) also displays the 12.0 ppm peak. Like the zirconia-bound monolayers, the ^{1}H NMR resonances of the pendant CO_2H groups appear to be broadened into the baseline. A 2D ^{1}H DQ MAS NMR spectrum of $HO_2C(CH_2)_{15}PO_3H_2/TiO_2$ is shown in Figure 4b. 2D ^{1}H DQ MAS NMR spectra consist of the single-quantum (SQ) dimensions plotted against the double-quantum dimensions (DQ). Peaks that fall along the diagonal (ω, 2ω) are autocorrelation peaks, while pairs of off-diagonal peaks at (ω_a, $\omega_a + \omega_b$) and (ω_b, $\omega_a + \omega_b$) correspond to correlations between two protons with different chemical shifts.[20] The 2D ^{1}H DQ MAS NMR spectrum of the $HO_2C(CH_2)_{15}PO_3H_2/TiO_2$ sample shows autocorrelation peaks for the

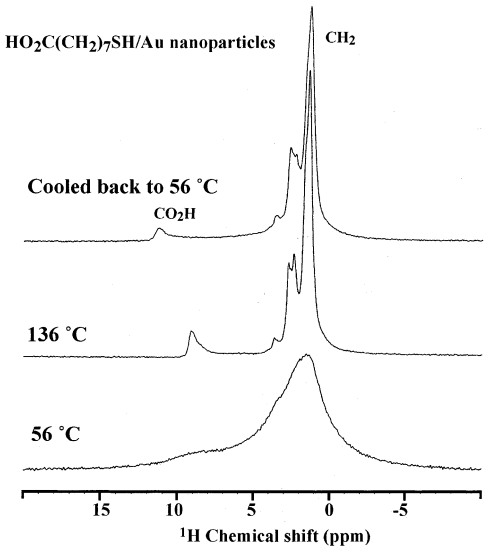

Figure 5. Variable temperature ^{1}H MAS NMR spectra of $HO_2C(CH_2)_7$-SH coated Au nanoparticles acquired at MAS spinning frequencies of 30 kHz.

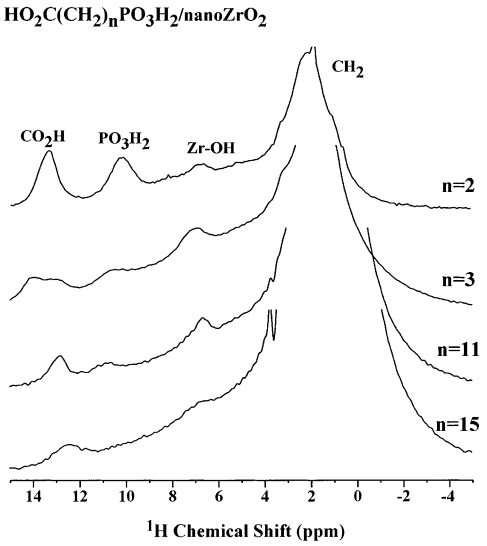

Figure 6. 1D ^{1}H DQ NMR spectra of $HO_2C(CH_2)_nPO_3H_2$, $n = 2$, 3, 11, 15, adsorbed on nanoZrO_2, acquired with MAS spinning frequencies of 30 kHz and DQ excitation times of 66 μs.

aliphatic and the P−OH protons. Depending on the binding state, the autocorrelation peak for the P−OH protons of the $HO_2C(CH_2)_{15}PO_3H_2/TiO_2$ sample may be due to inter- and/or intramolecular dipolar couplings because the adsorbed phosphonic acid group may contain two P−OH groups. The weak P−OH proton peak in the $HO_2C(CH_2)_nPO_3H_2/ZrO_2$ samples on the other hand did not give rise to a DQ signal, indicating that only isolated residual P−OH groups are present.

4.3. Variable Temperature ^{1}H MAS NMR of $HO_2C(CH_2)_7SH$/Au Nanoparticles. The assumption that the ^{1}H NMR resonances of the pendant carboxylic acid groups of the $HO_2C(CH_2)_nPO_3H_2/ZrO_2$ and TiO_2 samples are heterogeneously broadened beyond detection is supported by a ^{1}H fast MAS NMR study of an analogous monolayer system, $HO_2C(CH_2)_7$-SH coated gold nanoparticles. Unlike the SAMs on metal oxide substrates, there is no possibility for any ionic or hydrogen-bonding interactions of the carboxylic acid groups with the gold surface. Like the carboxyalkylphosphonate SAMs, infrared spectroscopy indicates that the terminal acid groups of the gold nanoparticles are extensively hydrogen-bonded.[27] The ^{1}H fast MAS NMR spectrum of the $HO_2C(CH_2)_7SH$/Au nanoparticles in Figure 5 shows that this hydrogen bonding is disordered because only a very broad shoulder at ∼8−10 ppm is visible in addition to the methylene peak. This shoulder is suppressed by a double-quantum filter. The broadness of the methylene proton peak relative to those of the $HO_2C(CH_2)_nPO_3H_2$ monolayers reflects the fact that the chain mobility of the carboxylic acid functionalized gold nanoparticles is quite restricted, approaching that of a rigid crystalline solid.[27] The CO_2H protons of the $HO_2C(CH_2)_7SH$/Au nanoparticles are clearly detected upon heating the sample above 120 °C for a prolonged period, as seen in Figure 5. New narrow peaks appear in both the aliphatic and the acidic proton regions. The new carboxylic acid proton peak broadened and shifted downfield from 9 to 12 ppm as the sample was slowly cooled. A mobile component remained, and examination of the sample after cooling revealed that some decomposition of the sample had occurred, with the presence of a white waxy solid in addition to the black $HO_2C(CH_2)_7SH$/Au nanoparticles. The new narrow peaks in the aliphatic region at 2.7−2.4 ppm have chemical shifts in the same range as the α methylene protons of disulfides (2.7 ppm) and/or thiols (2.5 ppm). The α methylene protons are normally noticeably absent in the solution ^{1}H spectra of alkanethiols bound to gold nanoparticles.[30] We propose that the surfactant comes off the nanoparticles primarily in the form of a disulfide due to oxidation during heating. Only when the surfactant is no longer surface-bound can the carboxylic acid groups rearrange to form head-to-head dimers and a more homogeneous bonding arrangement, giving rise to an observable CO_2H resonance. The shifting of a CO_2H proton peak between 9 and 12 ppm was also observed for hexabenzocoronene carboxylic derivatives heated to the liquid crystalline state.[26] In this study, the proton chemical shift of 9 ppm in the liquid crystalline state was attributed to free CO_2H groups which re-form hydrogen-bonded dimers upon cooling, returning to the original chemical shift of 12 ppm.[26] A similar process occurs for the CO_2H groups of the $HO_2C(CH_2)_7SH$/Au nanoparticles after the surfactant has been thermally desorbed from the gold particles. In contrast, the $HO_2C(CH_2)_nPO_3H_2/ZrO_2$ monolayers are thermally stable up to the highest temperature that the NMR probe can reach (∼140 °C) with only a reversible chain order/disorder process detected.[14] The ^{31}P NMR spectra show that the chains remained pinned to the surface during this process and no ^{1}H NMR peaks for the terminal CO_2H groups were detected.

4.4. $HO_2C(CH_2)_nPO_3H_2$ on ZrO_2 Nanopowder. (a) 1D ^{1}H DQ MAS NMR. The 1D ^{1}H DQ MAS NMR spectra of $HO_2C(CH_2)_nPO_3H_2$, $n = 2$, 3, 11, and 15, adsorbed on the ZrO_2 nanopowder (nanoZrO_2) are presented in Figure 6. In contrast to the lower surface area ZrO_2 and TiO_2 powders, the acid proton signals of the diacids adsorbed on the nanoZrO_2 are visible. Note also the splitting of the CO_2H proton resonance at ∼13 ppm in the $n = 3$ adsorbed diacid spectrum. The ^{31}P MAS NMR spectra of all of these samples contain narrow components between 24.5 and 27.7 ppm in addition to the very broad peak at ∼23−24 ppm assigned to the surface-bound phosphonate group.[14] Elemental analyses indicate the presence of diacid in

(30) Badia, A.; Singh, S.; Demers, L.; Cuccia, L.; Brown, G. R.; Lennox, R. B. *Chem.-Eur. J.* **1996**, *2*, 359−63.

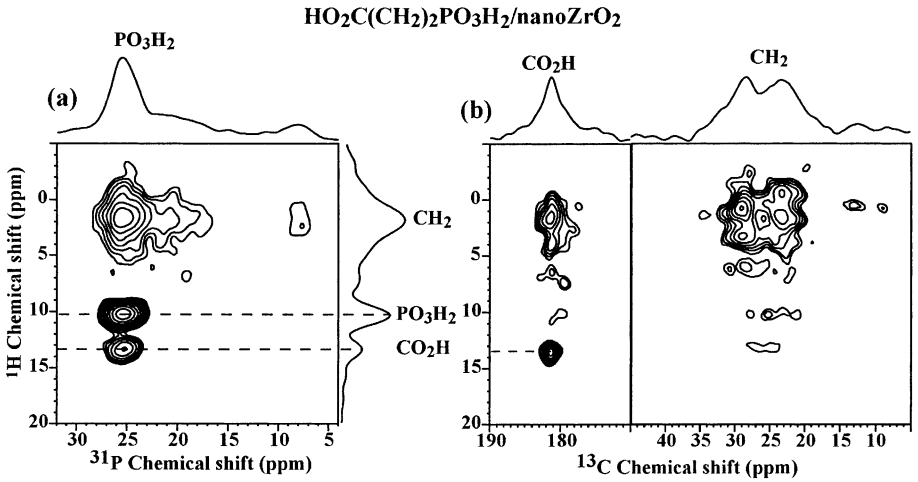

Figure 7. (a) 2D $^{1}H-^{31}P$ HETCOR NMR spectrum and (b) 2D $^{1}H-^{13}C$ HETCOR NMR spectrum of $HO_2C(CH_2)_2PO_3H_2$ adsorbed on nanoZrO_2 acquired with MAS spinning frequencies of 30 kHz and contact times of 100 μs and 2 ms, respectively.

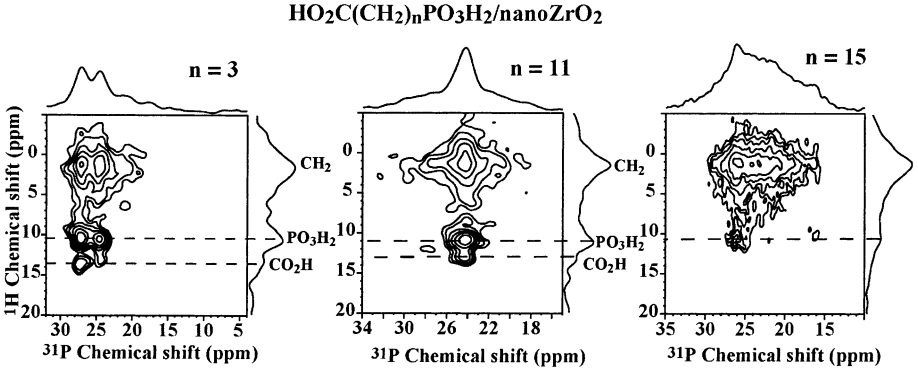

Figure 8. 2D $^{1}H-^{31}P$ HETCOR NMR spectra of $HO_2C(CH_2)_nPO_3H_2$, $n = 3$, 11, and 15, adsorbed on nanoZrO_2 acquired with MAS spinning frequencies of 30 kHz and contact times of 100 μs.

excess of a monolayer (see Table 1), especially in the case of the short chains, $n = 2$ and 3, which had estimated coverages of 248 and 182%, respectively. The excess diacid is strongly hydrogen-bonded to the pendant carboxylic acid groups of the surface-bound monolayer and cannot be removed by multiple washings with acetone. The deposition solvent, acetone, does not compete for hydrogen bonding, but when a small amount of water or methanol was used to wash the samples, the acidic proton resonances at 13.5 and 10.5 ppm vanished along with the narrow components in the ^{31}P NMR spectra.[14]

(b) 2D $^{1}H-X$ HETCOR NMR. Because the carboxylic and phosphonic acid ^{1}H chemical shifts may vary in the adsorbed state, 2D $^{1}H-X$ HETCOR NMR experiments were used to confirm the assignments. The 2D $^{1}H-^{31}P$ and $^{1}H-^{13}C$ HETCOR NMR spectra of $HO_2C(CH_2)_2PO_3H_2$/nanoZrO_2 are given in Figure 7. Only the $n = 2$ adsorbed diacid on the nanoZrO_2, which had a coverage of 248%, had sufficient signal sensitivity for a $^{1}H-^{13}C$ HETCOR NMR experiment. In contrast to the $^{1}H-^{31}P$ HETCOR NMR spectra of the bulk diacids (see Figure 2), significant correlations between the phosphorus signal and both acid protons at 10.5 and 13.5 ppm are present. These correlations are solely associated with the narrow ^{31}P component assigned to the excess diacid. Because the correlation to the ^{1}H signal at 10.5 ppm is more intense, this peak is assigned to the phosphonic acid group of the weakly bound excess diacid, and the peak at 13.5 ppm is assigned to the CO_2H protons. This assignment is confirmed from the $^{1}H-^{13}C$ HETCOR NMR spectrum of the $HO_2C(CH_2)_2PO_3H_2$/nanoZrO_2 sample, Figure 7b, which shows a correlation between the carbonyl carbon and the ^{1}H signal at 13.5 ppm. The correlation between the narrow phosphorus component and the carboxylic acid proton in the $^{1}H-^{31}P$ HETCOR NMR spectrum must be of intermolecular origin because no such correlation is observed for the bulk diacid using the same short contact time of 100 μs. Therefore, the spatial arrangement of the diacids in the adsorbed multilayers must be rearranged from that of the bulk state such that the CO_2H and PO_3H_2 groups are in close proximity. The small changes in the isotropic ^{1}H shifts of the CO_2H and PO_3H_2 protons in the multilayers (13.5 and 10.5 ppm) from the bulk values (13.0 and 11.0 ppm) would correspond to equal hydrogen-bond lengths of 2.62 Å for the carboxylic and phosphonic acid groups, slightly shorter than the bulk state values.[25]

The 2D $^{1}H-^{31}P$ HETCOR NMR spectra of the other carboxyalklphosphonates, $n = 3$, 11, and 15, adsorbed on the ZrO_2 nanopowder are shown in Figure 8. The 2D $^{1}H-^{31}P$ HETCOR NMR spectrum of the other short chain diacid, $n = 3$, is similar to the $n = 2$ diacid except that there are two narrow components in the ^{31}P dimension, assigned to two types of weakly bound diacid with slightly different surface hydrogen-bonding arrangements. The HETCOR spectrum shows that the two narrow ^{31}P components are associated with the splitting in the CO_2H ^{1}H NMR signal. The $HO_2C(CH_2)_{11}PO_3H_2$/nanoZrO_2 sample also contains some weakly bound diacid as seen from the narrow component in the ^{31}P dimension which shows small

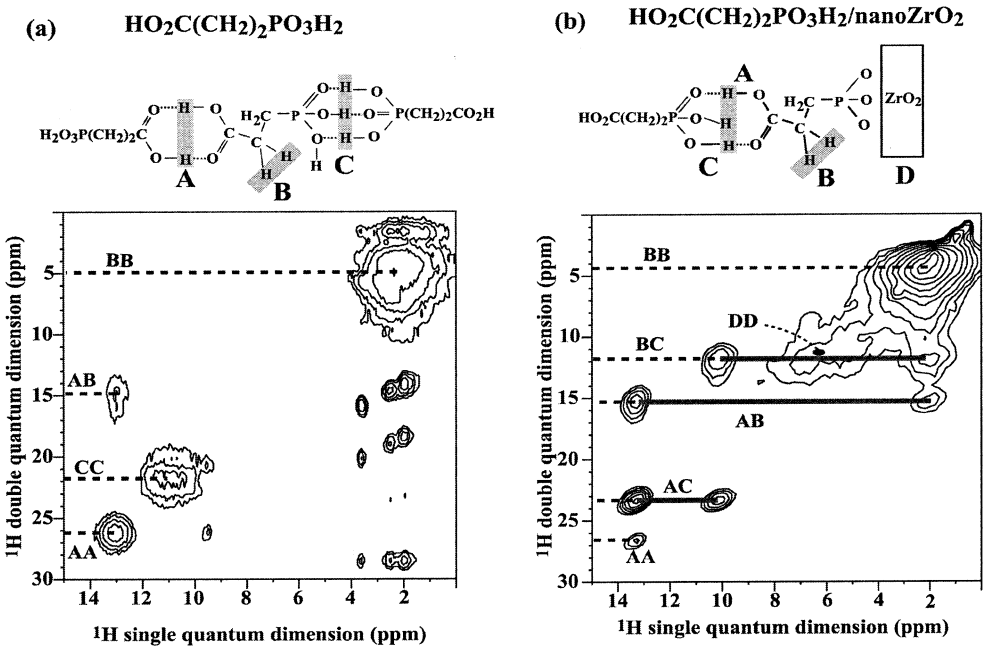

Figure 9. 2D ^{1}H DQ NMR spectra of $HO_2C(CH_2)_2PO_3H_2$ (a) in the bulk state and (b) adsorbed on nanoZrO_2 acquired with MAS spinning frequencies of 30 kHz and DQ excitation times of 66 μs.

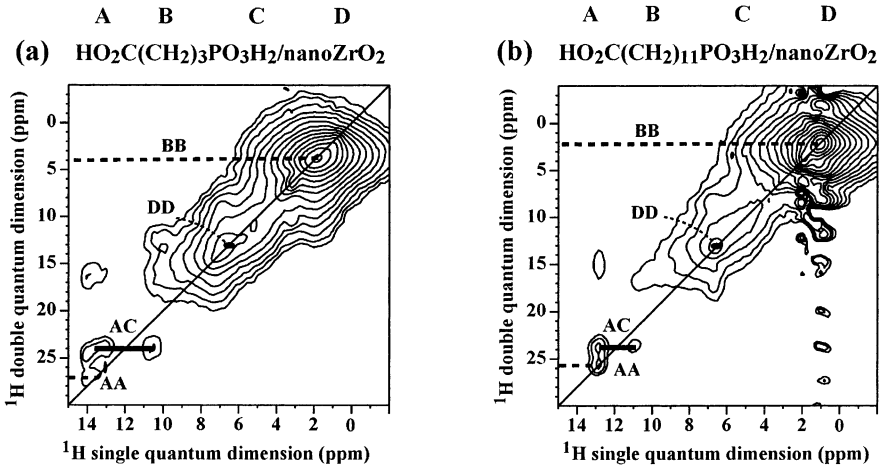

Figure 10. 2D ^{1}H DQ NMR spectra of (a) $HO_2C(CH_2)_3PO_3H_2$ and (b) $HO_2C(CH_2)_{11}PO_3H_2$ adsorbed on nanoZrO_2 acquired with MAS spinning frequencies of 30 kHz and DQ excitation times of 66 μs.

correlations to the carboxylic and phosphonic acid protons at 11 and 13 ppm. The ^{31}P spectrum of the longest chain sample, $HO_2C(CH_2)_{15}PO_3H_2$/nanoZrO_2, contains only a minuscule narrow ^{31}P component which shows a correlation only to the P−OH proton resonance at 11 ppm, indicating that all of the surfactant is directly bound to the metal oxide surface.

(c) 2D ^{1}H DQ MAS NMR. The 2D ^{1}H DQ MAS NMR spectra of the $HO_2C(CH_2)_nPO_3H_2$/nanoZrO_2 samples and the shortest and longest chain bulk diacids, $n = 2$ and 15, are presented in Figures 9−11. In addition to the autocorrelation peaks, the 2D ^{1}H DQ MAS NMR spectra of the bulk diacids (Figures 9a and 11a) contain a single off-diagonal peak at 13, 15 ppm, corresponding to a DQ coherence between a carboxylic acid proton and a methylene proton. Note that the companion cross-peak which should appear at 2, 15 ppm is missing. The absence of the companion cross-peak is commonly observed for DQ coherences associated with strongly dipolar coupled methylene protons.[20] The column of small peaks in the spectrum for the bulk short chain diacid, $n = 2$, is due to t_1 noise from adsorbed water and a residual mobile component. The t_1 noise arises from the loss of signal coherence caused by relaxation of the magnetization during the t_1 time increment.[20] The CO_2H autocorrelation peaks in the DQ spectra of the bulk diacids must originate from hydrogen-bonded head-to-head acid dimers, whereas the autocorrelation peak of the PO_3H_2 group may be both inter- and intramolecular in origin. The geometry of the hydrogen bonds of solid phenylphosphonic acid has recently been reported and shown to consist of PO_3H_2 dimers linked together by hydrogen bonds to form rings.[31] In addition to intramolecular DQ coherences between the two P−OH protons of the PO_3H_2 group, several types of intermolecular DQ coherences are possible if a similar network of linked dimers is formed by the phosphonic acid groups of the diacids. Because only autocorrelation peaks appear in the acid proton region, there must be only hydrogen-bonded homodimers in the bulk diacids. The ^{1}H−^{31}P HETCOR spectra of the bulk diacids (Figure 2)

(31) Mahmoudkhani, A. H.; Langer, V. *J. Mol. Struct.* **2002**, *609*, 97−108.

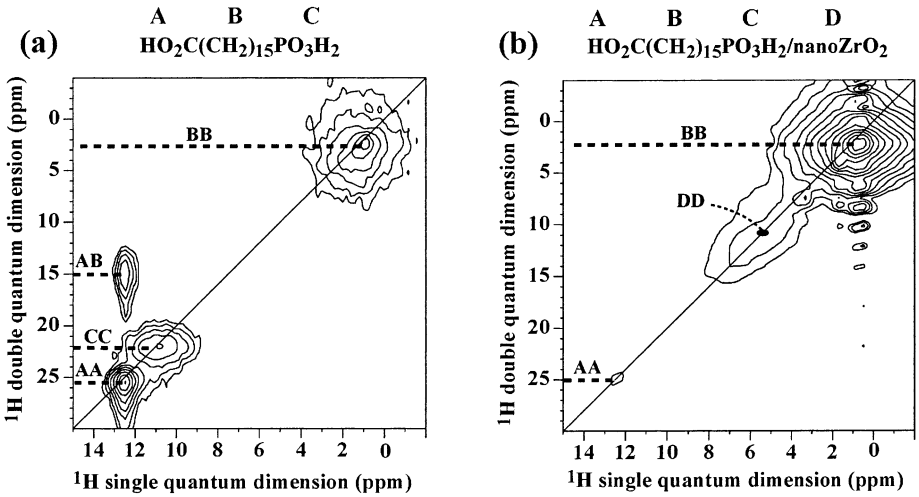

Figure 11. 2D ^{1}H DQ NMR spectra of $HO_2C(CH_2)_{15}PO_3H_2$ (a) in the bulk state and (b) adsorbed on nanoZrO_2 acquired with MAS spinning frequencies of 30 kHz and DQ excitation times of 66 μs.

further support the absence of hydrogen-bonding interactions between the carboxylic and phosphonic acid end groups because no correlations between the phosphate group and the carboxylic acid proton are detected at short contact times.

As seen in Figure 9b, a dramatic change in the 2D ^{1}H DQ MAS NMR spectrum of $HO_2C(CH_2)_2PO_3H_2$ occurs upon adsorption on the ZrO_2 nanopowder. Both peaks of the off-diagonal pairs corresponding to correlations between acid and methylene protons are now resolved, indicating a weakening of the methylene dipolar interactions, due to either an enhanced mobility and/or a less dense packing as compared to that of the bulk crystalline diacid. The autocorrelation peak for the carboxylic acid proton is much weaker, and that of the phosphonic acid is no longer visible (a weak PO_3H_2 autocorrelation peak was observed in some samples). A new pair of off diagonal peaks at 13, 23.5 ppm and 10.5, 23.5 ppm dominates the acid proton chemical shift region. These peaks correspond to a correlation between the carboxylic and phosphonic acid protons because the shift of 23.5 ppm in the double-quantum dimension is equal to the sum of the chemical shifts of the two acid groups. The appearance of the new DQ coherence between the two acid groups concurs with the close spatial proximity between the phosphorus group and the carboxylic acid protons detected by the ^{1}H$-^{31}$P HETCOR experiment. The excess diacid on the ZrO_2 nanopowder is hydrogen-bonded to the directly surface-bound monolayer in such a way to produce acid heterodimers rather than homodimers.

Weak off-diagonal signals are also detected in the ^{1}H DQ MAS NMR spectra of $HO_2C(CH_2)_nPO_3H_2$/nanoZrO_2, $n = 3$ and 11, given in Figure 10. When the $HO_2C(CH_2)_{11}PO_3H_2$/nanoZrO_2 was subjected to additional washes with warm methanol rather than acetone, the deposition solvent, the coverage decreased from 104 to 80%, and both the narrow ^{31}P NMR component and the off-diagonal peaks in the 2D ^{1}H DQ MAS NMR spectrum vanished. The 2D ^{1}H DQ MAS NMR spectra of the longest chain surfactant, $HO_2C(CH_2)_{15}PO_3H_2$, in the bulk and adsorbed state are shown in Figure 11. In contrast to the other samples, no off-diagonal peaks are observed in the acid region, and there is only a very weak autocorrelation peak at 12.5 ppm that is assigned to the carboxylic acid proton because this peak did not appear in the ^{1}H$-^{31}$ P HETCOR NMR spectrum (Figure 8).

5. Discussion

In this section, the results presented above are combined to construct a picture of the hydrogen-bonded structures formed by the adsorption of carboxyalkylphosphonic acids on ZrO_2 and TiO_2. ^{1}H MAS NMR techniques provide information about both the surface bonding and the intermolecular hydrogen-bonding interactions of the adsorbed diacids. Insight into the bonding of phosphonic acids on TiO_2 versus ZrO_2 is provided by the presence or absence of dipolar couplings among the P$-$OH protons. The possible sources for the disordered surface hydrogen bonding of the carboxylic acid terminated monolayers are examined. Last, evidence for the existence for acid heterodimers in the multilayers of the diacids on the ZrO_2 nanopowder is discussed.

5.1. Surface Bonding of Phosphonic Acids. The exact nature of the bonding state of phosphonic acids on metal oxides has not been well characterized. The phosphonate surface-binding mode may consist of tri-, bi-, or monodentate bonds, with the tri- or bidentate bonds in a bridging or chelating configuration, akin to what is shown in Figure 1a and b. Another possibility is that the phosphonic acid may just interact with the metal oxide surface via hydrogen-bonding interactions through the hydroxyl groups or oxo oxygen atoms (Figure 1c). Normally, the exact surface bond state cannot be extracted from FTIR spectroscopy due to the broad overlapping bands in the P$-$O stretching band region. The presence or absence of P$-$OH groups after adsorption is also difficult to determine from vibrational spectroscopy. Randon and co-workers detected the disappearance of the P$-$OH band at 940 cm^{-1} when phenylphosphonic acid was adsorbed on zirconia.[32] However, because the adsorption band of TiO_2 occurs in the same region, it was not possible to draw any conclusions about the bonding state of the same phosphonic acid on TiO_2. In a more recent study by Guerrero and co-workers, the broad TiO_2 signal was eliminated by subtracting a background spectrum. The attenuation of the P$-$OH band was noted, and the authors proposed that surface coordination of phosphonic acids on titania is primarily tridentate with some bidentate binding modes.[33] From the ^{31}P NMR spectra alone, one can only infer that adsorption has occurred,

(32) Randon, J.; Blanc, P.; Paterson, R. *J. Membr. Sci.* **1995**, *98*, 119−29.
(33) Guerrero, G.; Mutin, P. H.; Vioux, A. *Chem. Mater.* **2001**, *13*, 4367−73.

and no conclusions about the exact coordination state of the surface bond can be made from the changes in the chemical shift.[12,13] The ^{31}P NMR spectra of phosphonic acids adsorbed on titania versus zirconia are quite different in that the ^{31}P signal for phosphonic acid adsorbed on ZrO_2 is far more shifted and greatly broadened as compared to that of the unbound acid, an indication of the stronger adsorption on ZrO_2.[12,13]

The ^{1}H−^{31}P HETCOR NMR spectra of the adsorbed carboxyalkylphosphonic acids demonstrate that there are still P−OH protons on both ZrO_2 and TiO_2. In the case of zirconia, these signals are quite weak and do not survive a double-quantum filter, indicating that only isolated residual P−OH groups remain. By contrast, the 2D ^{1}H DQ MAS NMR spectra of carboxyalkylphosphonic acids adsorbed on TiO_2 show the presence of dipolar coupled P−OH protons. Given that two protons must be less than 3.5 Å apart to produce a double-quantum coherence,[20,21] there are two possible sources for the P−OH double-quantum coherences of the TiO_2 samples. If a significant fraction of the adsorbed phosphonic acid groups are still fully protonated, *intra*molecular double-quantum coherences can arise from the two P−OH protons of the PO_3H_2 group. Second, hydrogen-bonding interactions between neighboring adsorbed phosphonic acid groups may occur in such a way to give rise to *inter*molecular double-quantum coherences. Because phosphonic acids generally bind more weakly to TiO_2 as compared to ZrO_2, the presence of a significant population of P−OH groups is not surprising. Gawalt and co-workers reported that the stability of alkylphosphonate and carboxyalkylphosphonate monolayers on the native oxide surface of titanium films is greatly enhanced by annealing the monolayers after being deposited from solution but before solvent washing.[34] Without this annealing step, the authors found that most of the surfactant which had been deposited from solutions at ambient temperature was removed by the solvent washing. Guerrero and co-workers deposited phosphonic acids from solutions at ambient temperature onto titania powder followed by washing and drying under vacuum at 120 °C. From the infrared spectra, they concluded that the phosphonic acid binds via condensation reactions with the surface Ti−OH groups.[33] Our sample preparation represents an intermediate case in that the phosphonic acids were deposited from hot solution, then washed with solvent, so that a certain population of uncondensed P−OH groups may survive. The density of these remaining P−OH groups is such that dipolar couplings between pairs of P−OH protons are detected. Gawalt and co-workers suggest that the initially adsorbed monolayers assemble on the TiO_2 surface through hydrogen-bonding interactions among the phosphonic acid headgroups.[34] The detection of dipolar coupled P−OH groups supports the view that hydrogen-bonding interactions are involved in the assembly and surface attachment of phosphonic acids on TiO_2 (Figure 1a). The presence of only isolated P−OH groups on ZrO_2 points toward a bidentate or tridentate binding mode on this substrate through extensive condensation with the surface hydroxyl groups (Figure 1a).

5.2. Disordered Surface Hydrogen Bonds. Whereas the P−OH groups are detected on both zirconia and titania, the ^{1}H NMR resonances for the terminal CO_2H protons are completely broadened into the baseline. Carboxylic acid functionalized thiols on gold nanoparticles, where there is no possibility of the CO_2H groups interacting with the surface, also display an extremely broad CO_2H proton peak. Infrared spectroscopy shows that the terminal CO_2H groups of all of three systems are hydrogen-bonded, but the ^{1}H NMR spectra indicate that there must be a broad distribution of slightly different hydrogen-bonding modes. A resolved CO_2H peak which appears in the ^{1}H NMR spectra of the gold nanoparticles after thermal oxidation led to liberation of the surfactant from the surface. The acid groups of the now unbound surfactant are free to form a more uniform array of head-to-head dimers. A similar process does not occur in the carboxyalkylphosphonate monolayers, which are thermally stable, so the acid resonance remains heterogeneously broadened beyond detection.

As for the source of the disorder in the surface hydrogen bonding, the role of the substrate geometry must be considered. Both free and hydrogen-bonded carboxylic acid groups are observed in the infrared spectra of carboxylic-acid terminated thiol monolayers on flat gold substrates, but only hydrogen-bonded groups are found for the same monolayers on the gold nanoparticles.[27] In the case of nanoparticle substrates, both *intramonolayer* and *interparticle* hydrogen bonds are possible, which would give rise to a more extensive but also more disordered hydrogen-bonded network. The intramonolayer hydrogen bonding alone must be disordered because the CO_2H proton NMR peak is broad for monolayers on metal oxides with larger particle sizes where there is a low likelihood of interparticle hydrogen bonds. Given the surface roughness of powder substrates and of metal oxide surfaces, in general, there will be variation in the relative heights of the neighboring pendant CO_2H groups, and a broad distribution of slightly different hydrogen-bonding modes can be expected. One might likewise expect a population of non-hydrogen-bonded CO_2H groups for SAMs on rough surfaces due to this variation in relative heights and given the fact that such a population is detected for SAMs on flat substrates. Indeed the influence of the gold topography on the film permeability and surface pK_a of carboxylic acid terminated SAMs has been explained by more extensive hydrogen bonding as the substrate becomes smoother.[22] However, the infrared spectra of the carboxyalkylphosphonates adsorbed on metal oxide powders indicate that only hydrogen-bonded carboxylic acid groups are present despite the surface roughness.[14]

A mixture of hydrogen-bonding geometries, such as cyclic and acyclic dimers or linear polymeric structures, could contribute to the broadness of the acid proton resonances. Although an earlier study of carboxylic acid terminated SAMs proposed that "sideways" head-to-head dimers form by partial rotation of the acid groups about the $C_\alpha-C_{C=O}$ bond,[23] other studies conclude that only laterally hydrogen-bonded configurations are possible.[22] A recent study proposes that for steric reasons only acyclic dimers or linear polymeric structures are present in CO_2H terminated monolayers displaying a high degree of chain order and the presence of head-to-head dimers is associated with monolayers with disordered chains or bilayers.[19] Whereas the carboxyalkylphosphonate SAMs contain highly disordered, lateral hydrogen bonds, the broadness of the CO_2H proton resonance of the gold nanoparticles is probably due to a mixture of intramonolayer acyclic dimers and interparticle head-to-head dimers. Dimerization of carboxylic acid groups should

(34) Gawalt, E. S.; Avaltroni, M. J.; Koch, N.; Schwartz, J. *Langmuir* **2001**, *17*, 5736−8.

give rise to a double-quantum coherence, but the weak broad shoulder at 8−10 ppm assigned to the CO_2H groups in the ^1H NMR spectrum of the carboxylic acid functionalized gold nanoparticles did not give rise to a detectable autocorrelation peak. Depending on the efficiency of a particular recoupling pulse sequence, the DQ filter will attenuate the ^1H NMR signal as compared to the single-quantum spectrum without the filter. This signal reduction, combined with the already low intensity and broadness of the CO_2H proton signal in the single-quantum spectrum, likely precludes detection of the CO_2H dimers on the Au nanoparticles by ^1H DQ NMR.

5.3. Hydrogen Bonding in Multilayers. In contrast to the monolayers, the hydrogen-bonding network formed by multilayers of the diacids on the ZrO_2 nanopowder is more ordered as indicated by the appearance of narrow ^1H NMR peaks which survive a double-quantum filter. Unlike the terminal CO_2H groups of the SAMs, the excess diacid molecules can form hydrogen bonds in a less constrained fashion among themselves and with the terminal carboxylic acid groups of the directly surface-bound monolayers. However, the most interesting feature is that the hydrogen-bonded structures of the multilayers are quite different from the bulk diacids, which only show hydrogen-bonded homodimers, that is, CO_2H-CO_2H and $PO_3H_2-PO_3H_2$. The combination of the heteronuclear correlation and double-quantum NMR experiments conclusively shows that the CO_2H and PO_3H_2 groups are strongly associated in the multilayers. This information would be difficult to obtain, even in an indirect fashion, by other experimental means. The infrared spectra of the short chain diacids ($n = 2$ and 3) adsorbed on the nanopowder show two C═O bands for hydrogen-bonded carboxylic acid groups. In addition to the C═O band at 1716 cm^{-1}, which is also present in the monolayer samples, there is a more intense band at 1681−1685 cm^{-1} which may be associated with the heterodimers. However, the existence of heterodimers would not have been proposed from the infrared spectra alone. The dominant population of $CO_2H-PO_3H_2$ heterodimers is somewhat surprising given the large dimerization enthalpies of carboxylic acids (50−60 kJ mol^{-1}) that should favor the formation of homodimers. The preferential adsorption of the phosphonic acid groups changes the relative stiochiometry of free acid groups available for hydrogen bonding from equal numbers of PO_3H_2 and CO_2H groups to an excess of CO_2H groups. One possible configuration would have the phosphonic acid groups of the excess diacid hydrogen-bonded to the pendant carboxylic acid groups of the surface-bound monolayer in a head-to-tail fashion. The details of the proposed structure of the hydrogen-bonded multilayers of the short chain diacids, as derived from density functional calculations in combination with the NMR results, will be presented in a later publication.[24]

6. Summary

High-resolution ^1H solid-state NMR techniques were used to characterize surface hydrogen-bonding interactions in adsorbed carboxyalkylphosphonates of varying chain lengths on zirconia and titania. The detection of dipolar connectivities among the P−OH groups when these diacids are adsorbed on titania concurs with hydrogen-bonding interactions among the phosphate groups and a relatively weak binding state on this substrate. The broadening of the acid proton resonance of carboxylic acid terminated monolayers on gold nanoparticles and metal oxide powders points toward a highly disordered surface hydrogen-bonding network. The hydrogen-bonding network in multilayers of the diacids is more ordered but highly perturbed from the bulk state with the formation of heterodimers rather than homodimers. Finally, the results presented in this study demonstrate that high-resolution ^1H solid-state NMR techniques will be highly useful for identifying specific noncovalent interactions between organic adsorbates and functionalized surfaces.

Acknowledgment. The authors thank the Natural Sciences and Engineering Research Council of Canada (NSERC) and Le Fonds Québécois de la Recherche sur la Nature et les Technologies (FQRNT) for financial support.

JA029008U